

## Supporting Information

### Integration of Single Co Atoms and Ru Nanoclusters Boosts the Cathodic Performance of Nitrogen-Doped 3D Graphene towards Lithium–Oxygen Batteries

*Mingrui Liu<sup>a</sup>, Jing Li<sup>b</sup>, Bin Chi<sup>a</sup>, Long Zheng<sup>a</sup>, Yuexing Zhang<sup>c</sup>, Qinghua Zhang<sup>c</sup>, Tang Tang<sup>d</sup>, Lirong Zheng<sup>e</sup>, Shijun Liao<sup>a,\*</sup>*

---

\*Corresponding author, e-mail: [chsjliao@scut.edu.cn](mailto:chsjliao@scut.edu.cn), fax +86-20-87113586

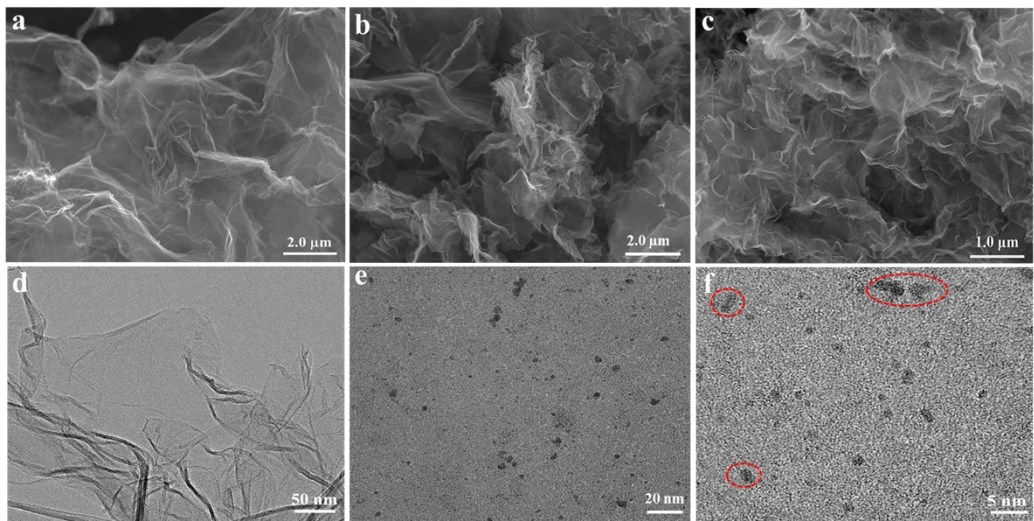


**Figure S1.** The SEM and TEM images of (a), (d) 3DNG, (b), (e) Co/ 3DNG, (c), (f) Ru<sub>NC</sub>/3DNG

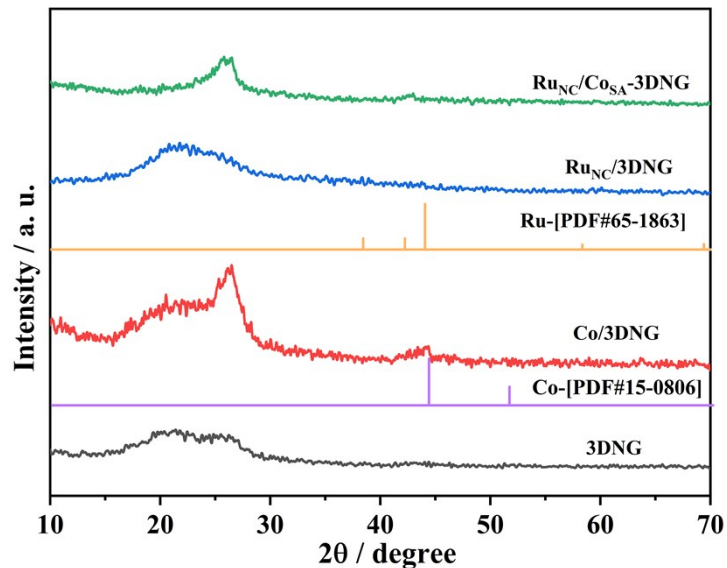


**Figure S2.** The XRD patterns of the 3DNG, Co/3DNG, Ru<sub>NC</sub>/3DNG and Ru<sub>NC</sub>/Co<sub>SA</sub>-3DNG samples.

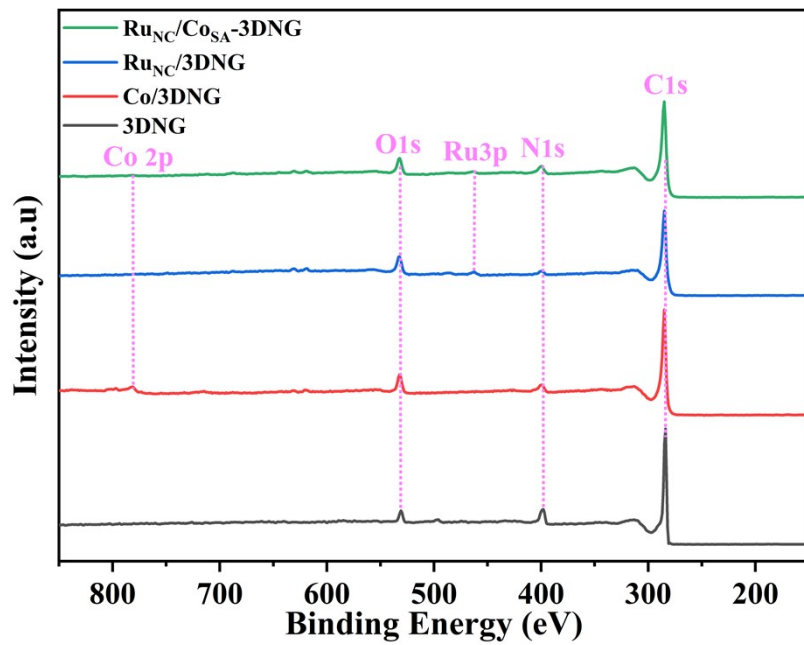


**Figure S3.** XPS survey spectra of 3DNG, Co/3DNG, Ru<sub>NC</sub>/3DNG and Ru<sub>NC</sub>/Co<sub>SA</sub>-3DNG.

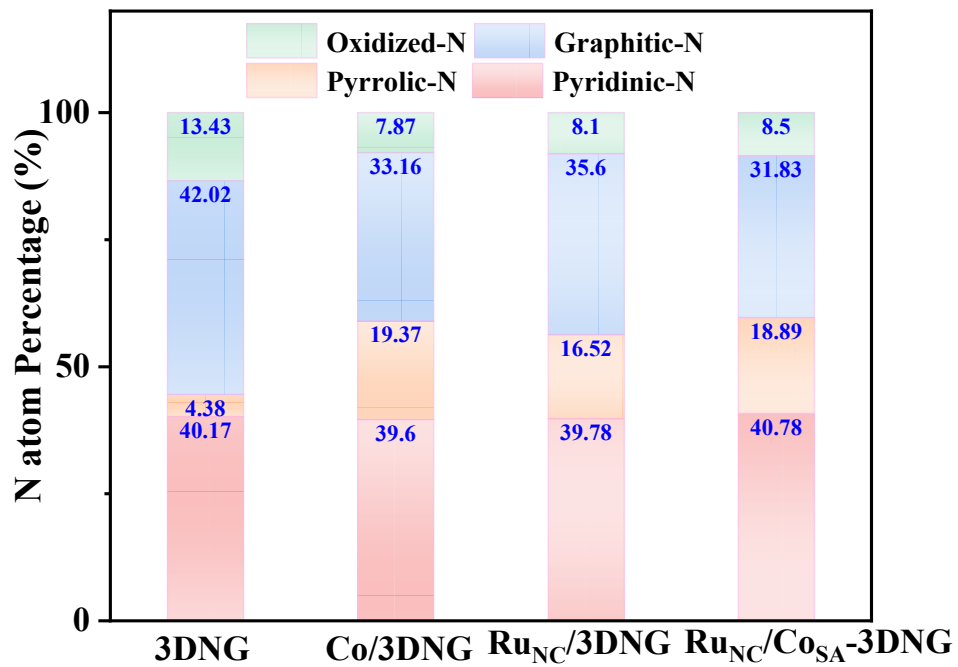


**Figure S4.** The distribution of the different N species.

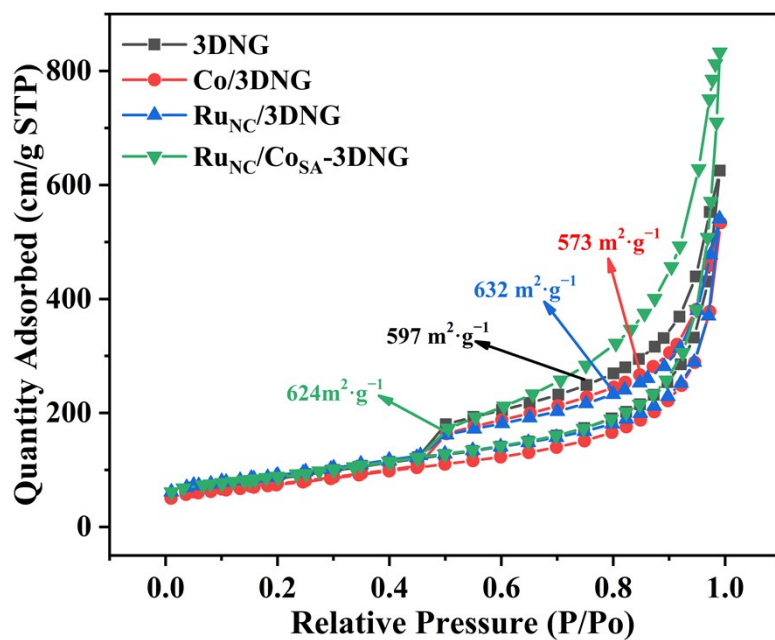


**Figure S5.** The nitrogen adsorption/desorption isotherms and pore size distribution of 3DNG, Co/3DNG, Ru<sub>NC</sub>/3DNG and Ru<sub>NC</sub>/Co<sub>SA</sub>-3DNG.

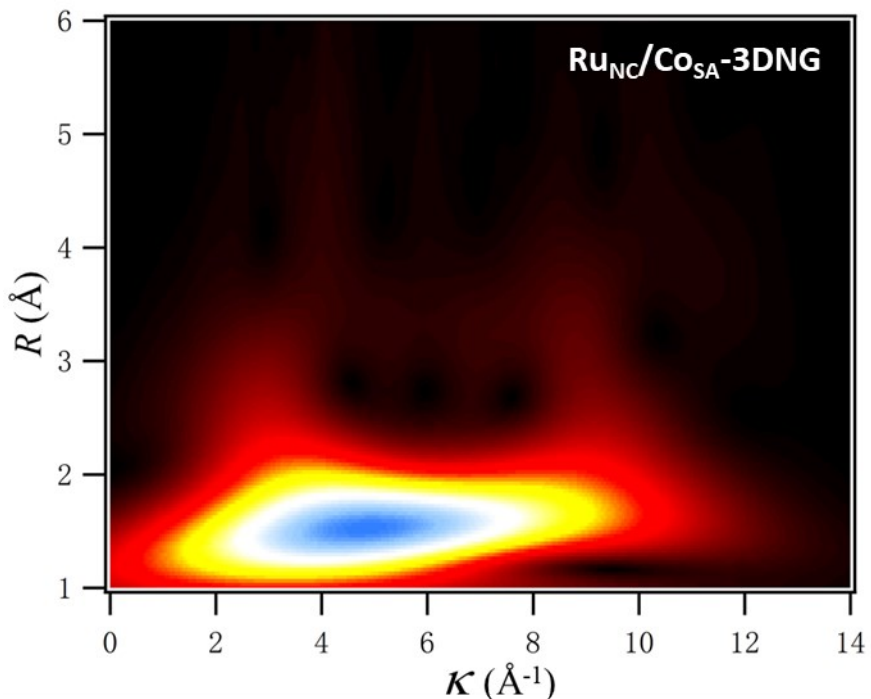


**Figure S6.** Wavelet transforms for the k<sup>3</sup>-weighted Co K-edge EXAFS signals of Ru<sub>NC</sub>/Co<sub>SA</sub>-3DNG. The maxima at 4.5 Å<sup>-1</sup> is associated with the Co-N contributions.

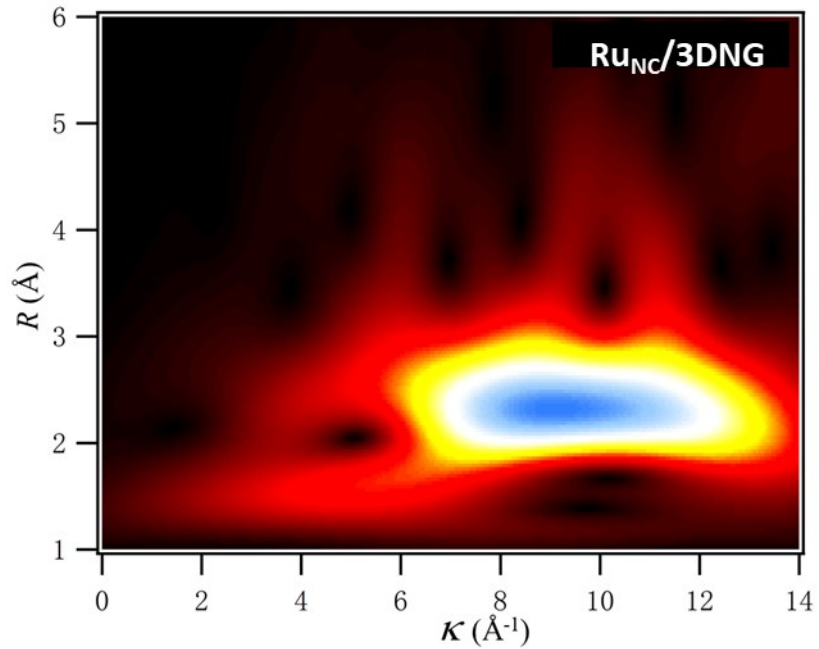


**Figure S7.** Wavelet transforms for the  $k^3$ -weighted Ru K-edge EXAFS signals of Ru<sub>NC</sub>/3DNG. Ru<sub>NC</sub>/3DNG shows a maximum at  $9.3 \text{ \AA}^{-1}$ , which indicates the dominance of metallic Ru nano crystallites.

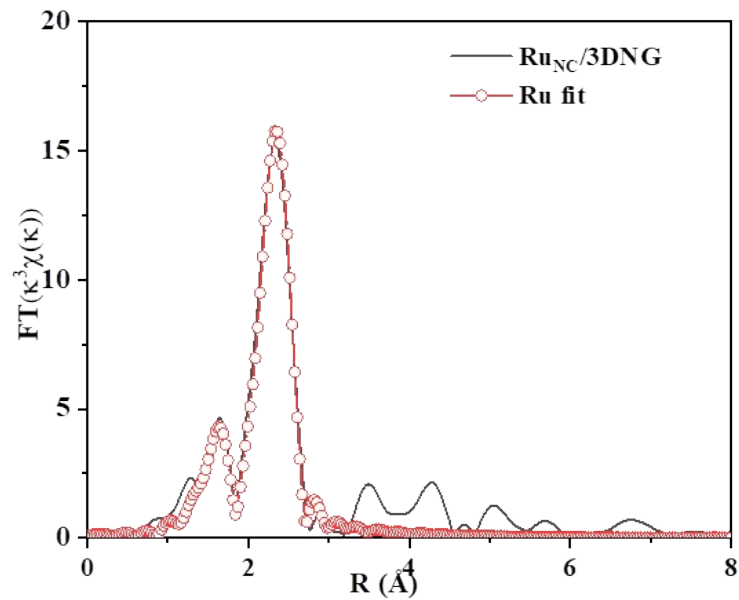


**Figure S8.** R space Fitting result of Ru K-edge of Ru<sub>NC</sub>/3DNG.

**Table S1.** EXAFS fitting results of Ru<sub>NC</sub>/Co<sub>SA</sub>-3DNG from Figure 3c-f

Sample	Shell	N <sup>a</sup>	R (Å) <sup>b</sup>	$\sigma^2$ (Å <sup>2</sup> ·10 <sup>-3</sup> ) <sup>c</sup>	$\Delta E_0$ (eV) <sup>d</sup>	R factor (%)
Ru <sub>NC</sub> /Co <sub>SA</sub> -3DNG	Co-N/O	6.0	2.08	9.1	0.3	0.3
	Co-Co	0.5	2.42	10.1	-0.2	
	Ru-N	4.1	2.05	7.8	3.5	1.3
	Ru-Ru	0.7	2.53	7.0	-0.6	
Ru <sub>NC</sub> /3DNG	Ru-N	1.3	2.02	1.4	-0.5	0.8
	Ru-Ru	6.4	2.67	6.7	-6.2	

<sup>a</sup>N: coordination numbers; <sup>b</sup> R: bond distance; <sup>c</sup>  $\sigma^2$ : Debye-Waller factors; <sup>d</sup>  $\Delta E_0$ : the inner potential correction. R factor: goodness of fit. S02 were set as 0.89/0.90 for Co-O/Co-Co, which were obtained from the experimental EXAFS fit of reference CoO/Co foil by fixing CN as the known crystallographic value and was fixed to all the samples. S02 were set as 0.85/0.90 for Ru-N/O, Ru-Ru, which were obtained from the experimental EXAFS fit of reference RuO<sub>2</sub>/Ru powder by fixing CN as the known crystallographic value and was fixed to all the samples.

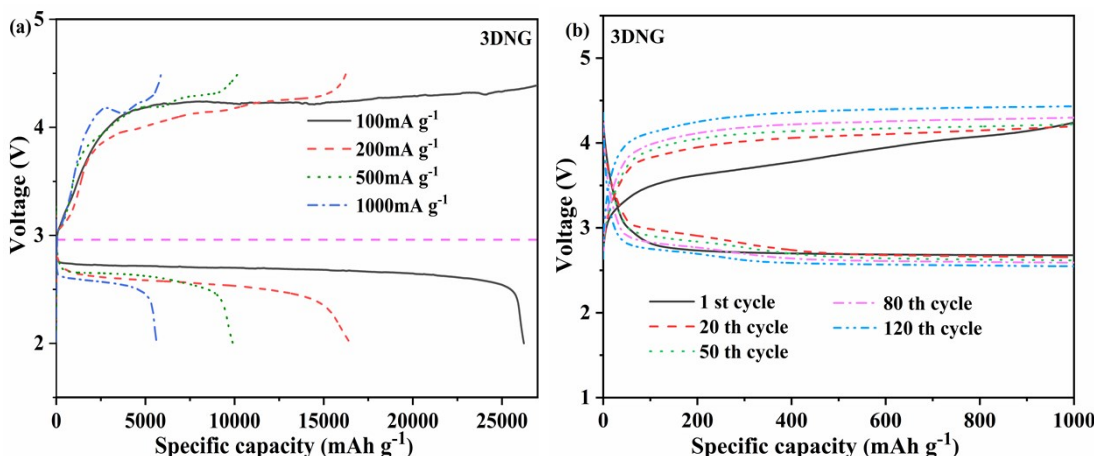


**Figure S9.** The rate performance of 3DNG cathode (2.0-4.5 V), and corresponding discharge-charge voltage profiles different cycles under specific capacity limit of 1000 mAh g<sup>-1</sup> at a rate of 200 mA g<sup>-1</sup>.

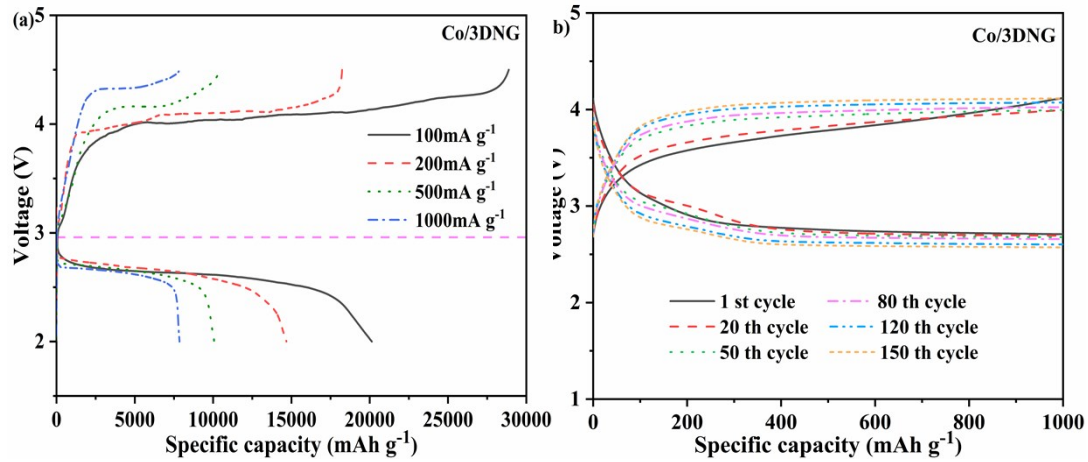


**Figure S10.** The rate performance of Co/3DNG cathode (2.0–4.5V), and corresponding discharge–charge voltage profiles different cycles under specific capacity limit of 1000  $\text{mAh g}^{-1}$  at a rate of 200  $\text{mA g}^{-1}$ .

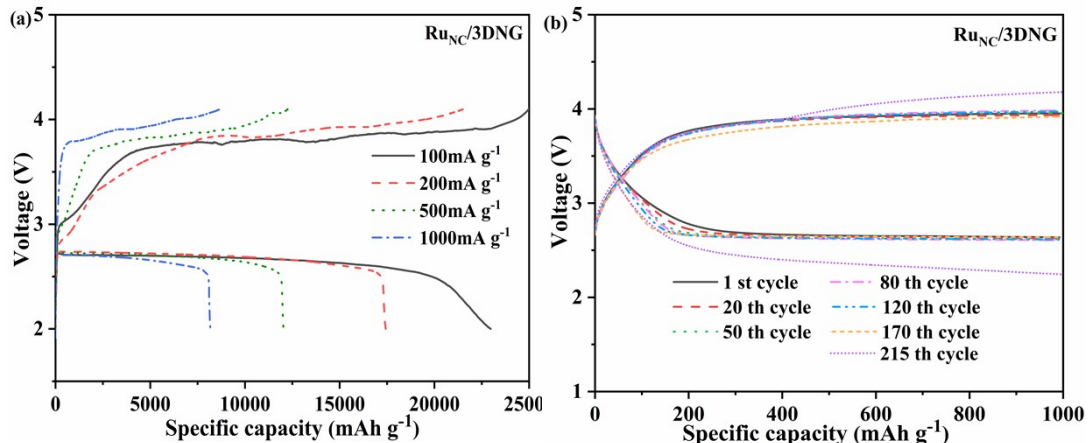


**Figure S11.** The rate performance of Ru<sub>NC</sub>/3DNG cathode (2.0–4.1V), and corresponding discharge–charge voltage profiles different cycles under specific capacity limit of 1000  $\text{mAh g}^{-1}$  at a rate of 200  $\text{mA g}^{-1}$ .

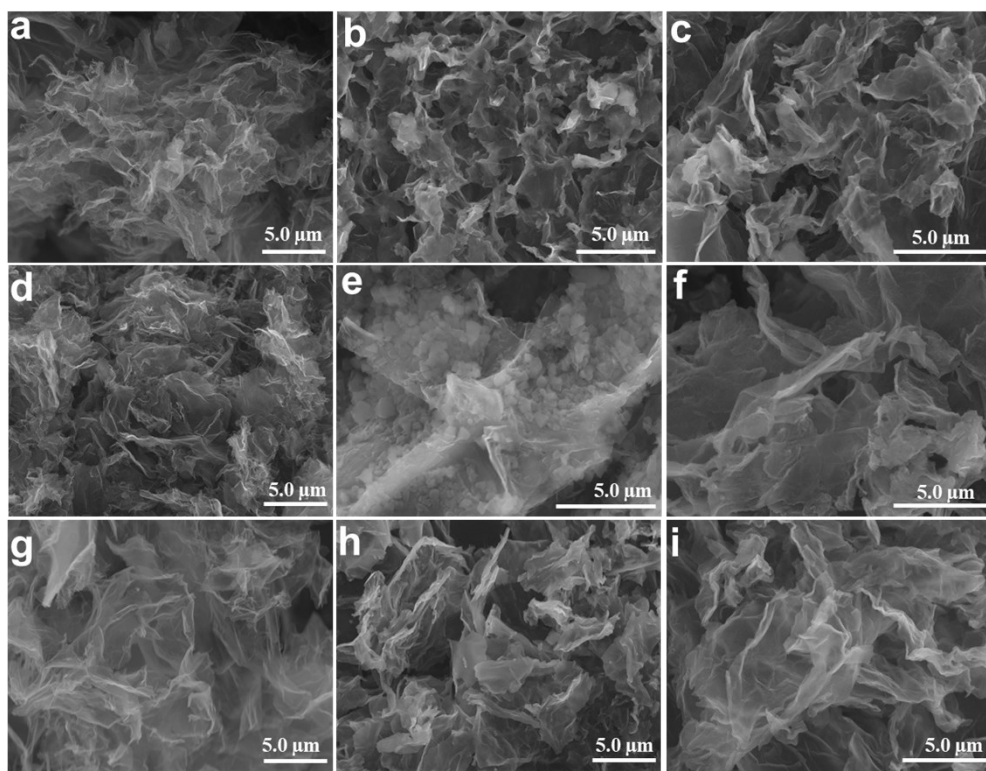


**Figure S12.** SEM images of pristine, discharged (2.0 V) and subsequent recharged (to 4.3V ) cathodes of 3DNG ( a, b, c ), Co/3DNG ( d, e, f ), Ru<sub>NC</sub>/3DNG ( g, h, I )

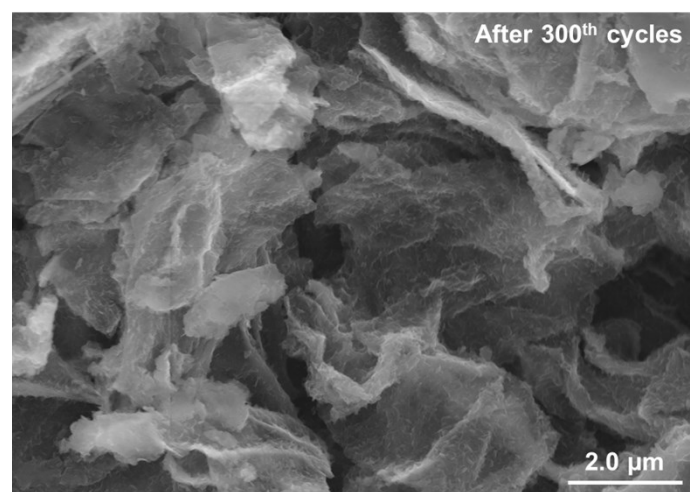


**Figure S13.** SEM images of Ru<sub>NC</sub>/Co<sub>SA</sub>-3DNG cathode after 300<sup>th</sup> cycles of discharge and charge process

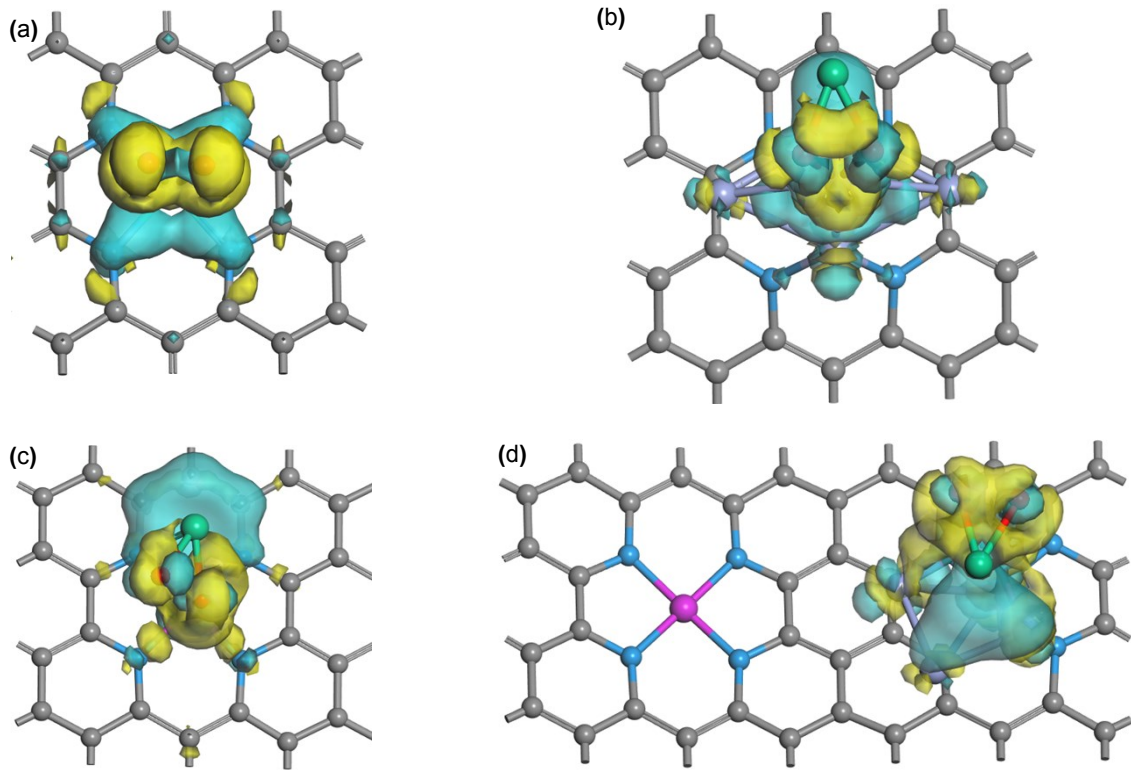


**Figure S14.** 3D plots of the charge density difference of the LiO<sub>2</sub> molecule adsorption on (a) 3DNG, (b) RuNC/3DNG, (c) single Co atoms and (d) Ru clusters of RuNC/CoSA-3DNG. The yellow and green isosurfaces represent the electron gain and lose, respectively. The corresponding isosurface value is 0.002 e/Bohr<sup>3</sup>.

**Table S2.** Comparison of specific capacity for various Ru/graphene-based cathodes.

Cathode	Mass loading (wt.%) )	Current density (mA/g)	Discharge Capacity (mAh/g)	overpotential	references
Ru@ Porous graphene	20.34	200	17700	0.35 V	[1]
Ru-graphene aerogels	18	0.1mA/cm <sup>2</sup>	12000	1.25 V	[2]
Ru@ VGNS@ Ni foam	43	200	23864	0.86 V	[3]
Ru-FeCoN/rGO	20	200	23905	~1.0 V	[4]
Ru@MPG	30	200	6433	~1.0 V	[5]
Ru/N-CNFs@TiO <sub>2</sub>	20.3	0.15 mA/cm <sup>2</sup>	2.0 mAh/m <sup>2</sup>	~0.94 V	[6]
Ru/3D-NrGO	9.37	200	18727	0.88 V	[7]
Ru QD/NHG	--	300	2700	1.04 V	[8]
Ru <sub>0.3</sub> SAs-NC	2.48	0.02mA/m <sup>2</sup>	13424	1.37 V	[9]

Ru@MWCNTP	9.0	500	~27000	1.04 V	[10]
<b>Ru<sub>NC</sub>/Co<sub>SA</sub>-3DNG</b>	<b>8.82</b>	<b>100</b>	<b>25632</b>	<b>0.84 V</b>	<b>This work</b>

**Table S3.** Comparison of cycling stability for various Ru/graphene-based cathodes.

Cathode materials	Current density (mA/g)	Discharge Capacity (mAh/g)	Cycling numbers	overpotential	references
Ru@ Porous graphene	200	1000	200	~0.94 V	[1]
Ru-graphene aerogels	0.1mA/cm <sup>2</sup>	500	50	~1.04 V	[2]
Ru@ VGNS@ Ni foam	200	1000	200	~0.23 V	[3]
Ru-FeCoN/rGO	200	600	300	~1.04 V	[4]
Ru@MPG	100	500	55	~1.24 V	[5]
Ru/N-CNFs@TiO <sub>2</sub>	500	1000	132	~1.24 V	[6]
Ru/3D-NrGO	200	1000	200	~1.04 V	[7]
Ru QD/NHG	300	500	20	~0.85 V	[8]
Ru <sub>0.3</sub> SAs-NC	0.02mA/m <sup>2</sup>	1000	60	~1.29 V	[9]
Ru@MWCNTP	500	5000	50	~1.31 V	[10]
<b>Ru<sub>NC</sub>/Co<sub>SA</sub>-3DNG</b>	<b>200</b>	<b>1000</b>	<b>300</b>	<b>~1.02 V</b>	<b>This work</b>

### References:

- [1] B. Sun, X. Huang, S. Chen, P. Munroe, G. Wang, Nano Lett. 2014, 14, 3145.
- [2] J. Jiang, P. He, S. Tong, M. Zheng, Z. Lin, X. Zhang, Y. Shi, H. Zhou, NPG Asia Materials 2016, 8, e239.
- [3] D. Su, D. Han Seo, Y. Ju, Z. Han, K. Ostrikov, S. Dou, H.-J. Ahn, Z. Peng, G. Wang, NPG Asia Materials 2016, 8, e286.
- [4] X. Zeng, C. You, L. Leng, D. Dang, X. Qiao, X. Li, Y. Li, S. Liao, R. R. Adzic, J. Mater. Chem. A 2015, 3, 11224.
- [5] X. Lin, Y. Cao, S. Cai, J. Fan, Y. Li, Q.-H. Wu, M. Zheng, Q. Dong, J. Mater. Chem. A 2016, 4, 7788.
- [6] J. Yang, H. Mi, S. Luo, Y. Li, P. Zhang, L. Deng, L. Sun, X. Ren, J. Power Sources

2017, 368, 88.

- [7] M. Liu, K. Sun, Q. Zhang, T. Tang, L. Huang, X. Li, X. Zeng, J. Hu, S. Liao, ACS Sustainable Chem. Eng. 2020, 8, 6109.
- [8] M. Nazarian-Samani, H.-D. Lim, S. Haghigat-Shishavan, H.-K. Kim, Y. Ko, M.-S. Kim, S.-W. Lee, S. F. Kashani-Bozorg, M. Abbasi, H.-U. Guim, D.-I. Kim, K.-C. Roh, K. Kang, K.-B. Kim, J. Mater. Chem. A 2017, 5, 619.
- [9] X. Hu, G. Luo, Q. Zhao, D. Wu, T. Yang, J. Wen, R. Wang, C. Xu, N. Hu, J. Am. Chem. Soc. 2020, 142, 16776.
- [10] F. Li, Y. Chen, D.-M. Tang, Z. Jian, C. Liu, D. Golberg, A. Yamada, H. Zhou, Energy Environ. Sci. 2014, 7, 1648.